

THE CHANDRA DEEP FIELD NORTH SURVEY. XI. X-RAY EMISSION FROM LUMINOUS INFRARED STARBURST GALAXIES

D.M. ALEXANDER,¹ H. AUSSSEL,² F.E. BAUER,¹ W.N. BRANDT,¹ A.E. HORNSCHMEIER,¹ C. VIGNALI,¹
 G.P. GARMIRE,¹ AND D.P. SCHNEIDER¹

¹Department of Astronomy & Astrophysics, 525 Davey Laboratory, The Pennsylvania State University, University Park, PA 16802

²Institute for Astronomy, 2680 Woodlawn Drive, Honolulu, HI 96822
 Draft version November 15, 2018

ABSTRACT

Using the 1 Ms *Chandra* Deep Field North and 15 μ m *ISOCAM* HDF-N surveys we find a tight correlation between the population of strongly evolving starbursts discovered in faint 15 μ m *ISOCAM* surveys and the apparently normal galaxy population detected in deep X-ray surveys. Up to 100% of the X-ray detected emission-line galaxies (ELGs) have 15 μ m counterparts, in contrast to 10–20% of the X-ray detected absorption-line galaxies and AGN-dominated sources. None of the X-ray detected ELGs is detected in the hard band (2–8 keV), and their stacked-average X-ray spectral slope of $\Gamma \approx 2.0$ suggests a low fraction of obscured AGN activity within the X-ray detected ELG population. The characteristics of the $z = 0.4$ –1.3 X-ray detected ELGs are consistent with those expected for M82 and NGC 3256-type starbursts; these X-ray detected ELGs contribute $\approx 2\%$ of the 0.5–8.0 keV X-ray background. The only statistical difference between the X-ray detected and X-ray undetected 15 μ m selected ELGs is that a much larger fraction of the former have radio emission.

Subject headings: infrared: galaxies — X-rays: galaxies — galaxies: active — galaxies: starburst

1. INTRODUCTION

Faint 15 μ m *ISOCAM* surveys have revealed a large population of strongly evolving luminous infrared (IR) starbursts at $z \approx 1$ (e.g., Aussel et al. 1999; Elbaz et al. 1999; Elbaz et al. 2002). The space density of these sources is an order of magnitude higher than that found for luminous IR starbursts in the local Universe (i.e., $z \lesssim 0.1$). Although these sources only account for a small fraction of the star-forming galaxy population, they are likely to contribute a significant fraction of the star-formation history of the Universe (e.g., Chary & Elbaz 2001; Elbaz et al. 2002).

In this Letter we use the 1 Ms *Chandra* Deep Field-North (CDF-N; Brandt et al. 2001b, hereafter Paper V) and *ISOCAM* HDF-N (Aussel et al. 1999, 2002) surveys to show that these strongly evolving luminous IR starbursts are identified with the population of apparently normal galaxies detected in deep X-ray surveys (e.g., Giacconi et al. 2001; Hornschemeier et al. 2001, hereafter Paper II; Brandt et al. 2001a, hereafter Paper IV). Previous cross-identification studies have shown that $\approx 20\%$ of the *ISOCAM* sources are AGN-dominated; however, few constraints have been placed on the larger fraction of *ISOCAM* sources that do not have obvious AGN activity (e.g., Paper II; Paper IV; Fadda et al. 2002). The primary focus of this paper is to place constraints on the X-ray properties of these sources. The Galactic column density toward the CDF-N is $(1.6 \pm 0.4) \times 10^{20} \text{ cm}^{-2}$ (Stark et al. 1992), and $H_0 = 65 \text{ km s}^{-1} \text{ Mpc}^{-1}$, $\Omega_M = \frac{1}{3}$, and $\Omega_\Lambda = \frac{2}{3}$ are adopted throughout this Letter.

2. INFRARED AND X-RAY OBSERVATIONS

The 1 Ms CDF-N observations were centered on the HDF-N (Williams et al. 1996) and cover $\approx 450 \text{ arcmin}^2$ (Paper V). The $\approx 21.5 \text{ arcmin}^2$ region of the CDF-N survey coincident with

the 15 μ m *ISOCAM* observations is close to the CDF-N aim point. Forty-nine high-significance X-ray sources (i.e., WAVDETECT false-positive probability threshold of 10^{-7}) are detected in this area down to on-axis 0.5–2.0 keV (soft-band) and 2–8 keV (hard-band) flux limits of $\approx 3 \times 10^{-17} \text{ erg cm}^{-2} \text{ s}^{-1}$ and $\approx 2 \times 10^{-16} \text{ erg cm}^{-2} \text{ s}^{-1}$, respectively (Paper V).

The *ISOCAM* observations were performed at 6.7 μ m and 15 μ m. Because of the significantly smaller field-of-view of the 6.7 μ m observations and the small number of sources detected, only the 15 μ m observations are considered here. Discrete sources are detected down to $f_{15\mu\text{m}} \approx 20 \mu\text{Jy}$, although the *ISOCAM* observations are far from complete at this depth. In this study we focus on the 41 sources with $f_{15\mu\text{m}} \geq 100 \mu\text{Jy}$ in the complete 15 μ m selected sample of Aussel et al. (2002).

3. THE INFRARED-X-RAY CONNECTION

3.1. Basic source properties

Optical (*I*-band) sources taken from the photometric catalog produced in Alexander et al. (2001b, hereafter Paper VI) were matched to X-ray and 15 μ m sources using matching radii of $1''$ and $3''$, respectively (see Paper VI; Aussel et al. 2002).¹ The 15 μ m sources have $I = 18$ –23, and all but one source have redshifts in the catalogs of Cohen et al. (2000), Cohen (2001) or Dawson et al. (2001). By contrast, $\approx 40\%$ of the X-ray sources in the 15 μ m *ISOCAM* region have $I \geq 23$, although all but two of the $I < 23$ sources have redshifts.

In total 14 of the 41 15 μ m sources have X-ray counterparts in the high-significance X-ray source catalog.² However, given the comparatively low source density of 15 μ m sources, we can search for lower significance X-ray sources associated with 15 μ m sources without introducing a significant number of spurious X-ray detections. We ran WAVDETECT with a false-positive probability threshold of 10^{-5} and found six further

¹ The *I*-band photometric catalog was produced using the Barger et al. (1999) image publicly available from <http://www.ifa.hawaii.edu/~cowie/hdf/hdf.html>.

² X-ray sources detected in the soft band (0.5–2.0 keV), hard band (2–8 keV) or full band (0.5–8.0 keV) are matched to 15 μ m counterparts.

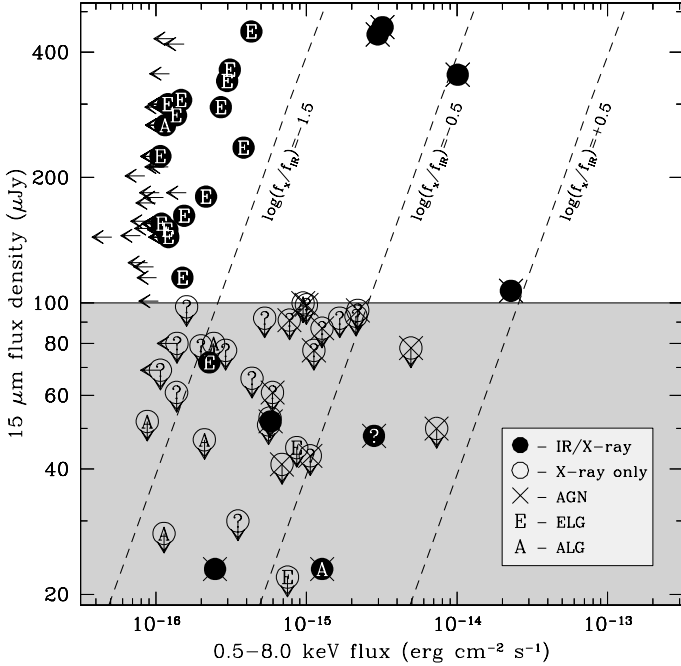


FIG. 1.— Full-band X-ray flux versus $15\ \mu\text{m}$ flux density. The filled circles are the X-ray-IR matched sources, and the open circles are the X-ray-only sources. Characters inside the circles indicate different source types: “E” indicates ELGs, “A” indicates ALGs, “?” indicates sources that do not have spectroscopic classifications, and overlaid crosses indicate AGN-dominated sources; see §3.2. IR sources not detected with X-ray emission are plotted only as upper limit arrows. The diagonal lines indicate constant flux ratios and the unshaded region indicates the IR sources that lie within the $15\ \mu\text{m}$ sample definition.

matches to $15\ \mu\text{m}$ sources; we would expect ≈ 0.01 of these six X-ray sources to be spurious. Finally, we calculated X-ray upper limits for the 21 X-ray undetected $15\ \mu\text{m}$ sources following §3.2.1 of Paper V. The fraction of $15\ \mu\text{m}$ sources with X-ray counterparts is $49^{+14}_{-11}\%$ (see Figure 1).³

We also matched the X-ray sources to the $15\ \mu\text{m}$ sources in the fainter $15\ \mu\text{m}$ sample of Aussel et al. (1999) and computed $15\ \mu\text{m}$ 3σ upper limits for all the X-ray sources without $15\ \mu\text{m}$ counterparts following Aussel et al. (2002). Five X-ray sources have $15\ \mu\text{m}$ detected counterparts with $f_{15\mu\text{m}} < 100\ \mu\text{Jy}$ (see Figure 1); these $15\ \mu\text{m}$ sources fall below our sample threshold and are not included in any further discussion.

3.2. Source-type classification

We have classified our sources since AGN-dominated sources are predicted to have different X-ray-to-IR flux ratios than non-AGN dominated sources (see Barcons et al. 1995; Alexander et al. 2001a). We adopt three source-type classifications: AGN-dominated sources, emission-line galaxies (ELGs), and absorption-line galaxies (ALGs). We considered a source to be AGN-dominated if it has either a “Q” (i.e., broad emission lines) optical spectral classification from Cohen et al. (2000), a rest-frame 0.5–8.0 keV

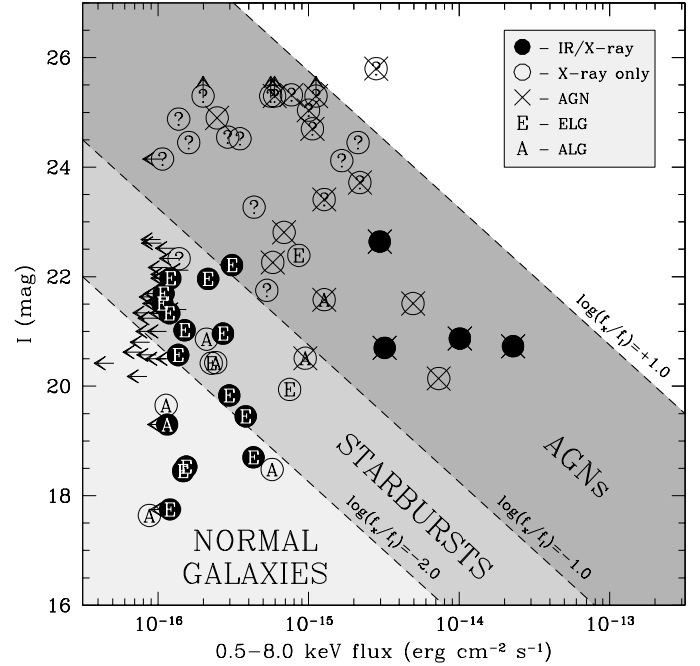


FIG. 2.— Full-band X-ray flux versus I -band magnitude. All symbols have the same meaning as in Figure 1. The diagonal lines indicate constant flux ratios. The shaded regions show the flux ratios of the AGN-dominated sources, X-ray detected starbursts and X-ray detected normal galaxies (see §3.3 and §4 for justification); these regions should be considered approximate.

luminosity $> 3 \times 10^{42}\ \text{erg s}^{-1}$, or a flat effective X-ray spectral slope (i.e., $\Gamma < 1.0$, an indicator of obscured AGN activity).^{4,5} Clearly there can be AGN-dominated sources not selected by these criteria (e.g., an AGN with $\Gamma > 1.0$ and a rest-frame 0.5–8.0 keV luminosity $< 3 \times 10^{42}\ \text{erg s}^{-1}$). We considered a source to be an ELG if it is not AGN dominated and has a classification including an “E” or “T” in Cohen et al. (2000). All sources with an “A” classification in Cohen et al. (2000) are considered ALGs; ALGs comprise both elliptical and quiescent spiral galaxies and can be AGN dominated.

3.3. AGN-dominated sources

In Figure 2 we show the full-band X-ray flux versus I -band magnitude for all of the $15\ \mu\text{m}$ and X-ray detected sources. Almost all of the 19 AGN-dominated sources have $\log(\frac{f_X}{f_I}) > -1$, consistent with the findings from previous X-ray surveys (e.g., Schmidt et al. 1998; Akiyama et al. 2000). Four AGN-dominated sources have $15\ \mu\text{m}$ counterparts. The resulting fraction ($21^{+18}_{-11}\%$) is consistent with that found by Fadda et al. (2002) and should be considered an upper limit since many of the unclassified sources with $\log(\frac{f_X}{f_I}) > -1$ are probably also AGN dominated. These four AGN-dominated sources are among the X-ray brightest sources (i.e., full-band fluxes $> 2 \times 10^{-15}\ \text{erg cm}^{-2}\ \text{s}^{-1}$). Assuming the highest X-ray-to-IR flux ratio of these AGN-dominated sources [i.e.,

³ All errors are taken from Tables 1 and 2 of Gehrels (1986) and correspond to the 1σ level; these were calculated assuming Poisson statistics.

⁴ All X-ray luminosities in this paper are calculated conservatively assuming $\Gamma = 2.0$ and no intrinsic or Galactic absorption.

⁵ When determining if a source has a flat X-ray spectral slope, we only considered sources bright enough to place meaningful constraints (see §3.2.1 in Paper V).

$\log(\frac{f_X}{f_{IR}}) \approx 0.5]$, an AGN-dominated source at the X-ray flux limit of our survey will have $f_{15\mu m} \approx 1 \mu\text{Jy}$; see §4 for discussion of deeper IR observations.

3.4. Emission-line galaxies

Fifteen of the 18 X-ray detected ELGs have $15 \mu\text{m}$ counterparts; see Figure 2. The three sources not detected at $15 \mu\text{m}$ have distinctive properties suggesting that their X-ray emission may well be AGN dominated. For example, all three sources have hard-band counterparts while none of the 15 sources detected at $15 \mu\text{m}$ has a hard-band counterpart. Furthermore, one of the three sources has an X-ray-to-optical flux ratio typical of an AGN-dominated source while another source is only detected in the hard band, suggesting it contains an obscured AGN.⁶ These three $15 \mu\text{m}$ undetected sources are excluded from further analysis of the X-ray detected ELGs as they are probably AGN dominated. Therefore, our results suggest that up to 100% of the X-ray detected ELGs (without AGN) have $15 \mu\text{m}$ counterparts. Since $15 \mu\text{m}$ detected ELGs only account for $\approx 20\%$ of the $R < 23.5$ ELG population in this region [as determined from the Cohen et al. (2000) data], this implies an association between the production of X-ray and IR emission in these sources.

All of the X-ray detected ELGs have faint X-ray emission (i.e., full-band fluxes $< 5 \times 10^{-16} \text{ erg cm}^{-2} \text{ s}^{-1}$), showing clear differences in the X-ray-to-IR and X-ray-to-optical emission relationships of AGN-dominated sources and X-ray detected ELGs (see Figures 1 and 2). While these sources are clearly not AGN-dominated, a fraction may contain a hidden (i.e., obscured) AGN as revealed by a flat X-ray spectral slope. Although none of the sources is detected in the hard band, we can stack the individual non-detections to provide a statistical constraint following §3.3 of Paper VI. This provides a detection in the hard band corresponding to an average band ratio (the ratio of hard-band to soft-band count rate) of 0.21 ± 0.04 , corresponding to an effective photon index of $\Gamma \approx 2.0$. To help interpret this result, we also stacked the 17 optically faint (i.e., $I \geq 24$) X-ray sources in Paper VI with full-band fluxes $< 5 \times 10^{-16} \text{ erg cm}^{-2} \text{ s}^{-1}$; the majority of these sources are thought to be obscured AGN. The average band ratio from this stacking analysis is $0.62^{+0.09}_{-0.08}$ ($\Gamma \approx 1.3$), substantially higher than that found for the ELGs. The reason for this difference is clear: $59^{+25}_{-18}\%$ of the optically faint X-ray sources have hard-band detections. Since we applied the same full-band flux limit to both samples, and thus took into account the high hard-band background, these results suggest a low fraction of obscured AGN within the ELG sample.

3.5. Absorption-line galaxies

Only one ($13^{+30}_{-11}\%$) of the eight X-ray detected ALGs has a $15 \mu\text{m}$ counterpart, in stark contrast to the higher $15 \mu\text{m}$ matching fraction found for the X-ray detected ELGs; see Figure 2. This difference could be due to either enhanced X-ray emission (e.g., an AGN component) or decreased IR emission (e.g., a weaker dust-emission component). Indeed, two ALGs are classified as AGN-dominated (see Figure 2), and the radio properties of a further fraction also indicate AGN activity (Bauer et al. 2002). However, if the absence of $15 \mu\text{m}$ counterparts in the other sources is due to a weaker dust-emission component, then their $15 \mu\text{m}$ emission is likely to be dominated by

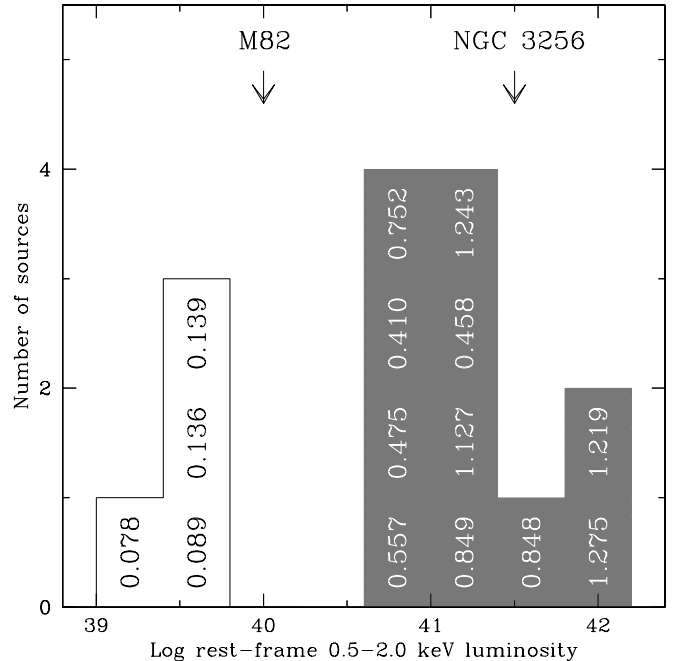


FIG. 3.— Rest-frame soft-band X-ray luminosity histogram for the X-ray detected ELGs with $15 \mu\text{m}$ counterparts. Individual source redshifts are shown (compare to Figure 2 in Paper VIII). The soft-band X-ray luminosities of the starburst galaxies M82 and NGC 3256 are indicated. The apparently bi-modality in the X-ray luminosities of the normal galaxies (unshaded) and starburst galaxies (shaded) is due to the small number of objects investigated here.

starlight. Following §3.4.3 of Alexander et al. (2002), the estimated $15 \mu\text{m}$ flux densities from starlight for these sources are $5\text{--}40 \mu\text{Jy}$, below the flux threshold of the $15 \mu\text{m}$ sample. Direct evidence for starlight emission is found in one source that is detected at $6.7 \mu\text{m}$ but not at $15 \mu\text{m}$ (CXO-HDFN J123649.5+621345; see Paper IV). Our estimated $15 \mu\text{m}$ flux density ($f_{15\mu m} = 40 \mu\text{Jy}$) is consistent with the upper limit for this source ($f_{15\mu m} < 52 \mu\text{Jy}$).

4. DISCUSSION

Studies of the faint $15 \mu\text{m}$ source population have shown that these sources are mostly luminous IR starburst galaxies undergoing intense dust-enshrouded star-formation activity that is re-radiated at IR wavelengths (e.g., Chary & Elbaz 2001). By cross-identifying the sources detected in the 1 Ms CDF-N and $15 \mu\text{m}$ ISOCAM HDF-N surveys, we have shown that this starburst population is associated with the population of apparently normal galaxies detected at faint X-ray fluxes (e.g., Giacomini et al. 2001; Paper II; Paper VI). With small X-ray-to-optical and X-ray-to-IR flux ratios [i.e., $\log(\frac{f_X}{f_I}) \lesssim -1$ and $\log(\frac{f_X}{f_{IR}}) < -1.5$, respectively], these X-ray detected ELGs are clearly different from AGN-dominated sources. None of the X-ray detected ELGs is detected in the hard band (2–8 keV), and their stacked-average X-ray spectral slope of $\Gamma \approx 2.0$ suggests a low fraction of obscured AGN activity within the X-ray detected ELG population.

⁶ This latter source was not bright enough to place meaningful constraints on its X-ray spectral slope (see §3.2.1 in Paper V).

The range of rest-frame soft-band luminosities for the 11 $z = 0.4\text{--}1.3$ X-ray detected ELGs suggests they are probably X-ray detected starburst galaxies similar to M82 and NGC 3256 (see Figure 3; e.g., Griffiths et al. 2000; Lira et al. 2002). The most X-ray luminous sources are up to ≈ 3 times more luminous than NGC 3256, the most X-ray luminous nearby starburst galaxy. The range of $\nu L_{15\mu\text{m}}$ luminosities ($\approx 2 \times 10^{10}$ to $\approx 2 \times 10^{12} L_{\odot}$ depending on the K -correction used; e.g., Elbaz et al. 2002) are also consistent with M82 and NGC 3256-type starbursts.⁷ Moran, Lehnert, & Helfand (1999) predicted that X-ray detected starbursts would contribute $\approx 5\text{--}30\%$ of the X-ray background (XRB). However, the total soft and hard band fluxes of the X-ray detected starbursts in this study ($7.7 \times 10^{-16} \text{ erg cm}^{-2} \text{ s}^{-1}$ and $1.5 \times 10^{-15} \text{ erg cm}^{-2} \text{ s}^{-1}$, respectively) only account for $\approx 2\%$ of the XRB (assuming the XRB flux densities given in Garmire et al. 2002). This fraction is below the lower limit given by Moran et al. (1999), although we note that these X-ray observations have probably not fully resolved the XRB (e.g., Cowie et al. 2002) and we might expect these sources to dominate the faint X-ray source counts.

The large fraction of X-ray detected ELGs with $15 \mu\text{m}$ counterparts suggests an association between the production of X-ray and IR emission. Since the $15 \mu\text{m}$ emission is considered an unobscured indicator of star-formation rate (e.g., Rowan-Robinson et al. 1997), this further suggests that the X-ray emission can provide an indication of star-formation rate. However, we urge caution since the 17 $15 \mu\text{m}$ detected ELGs undetected at X-ray energies have I -band magnitude, $I - K$ color, $V - I$ color, $15 \mu\text{m}$ flux density, and redshift distributions indistinguishable from the 11 X-ray detected starbursts (a Kolmogorov-Smirnov test gives probabilities of 98%, 97%, 48%, 78% and 55%, respectively).⁸ These results suggest a broad range of

X-ray luminosities for starbursts of similar IR luminosities and implies that there may be another factor that effects the production of the X-ray emission. The lack of a statistical difference between the $V - I$ and $I - K$ colors suggest that galaxy type and dust extinction effects are not important. However, we note that a much larger fraction of the X-ray detected starbursts have radio counterparts; see Bauer et al. (2002) for further constraints.

The four $z < 0.2$ sources have X-ray luminosities typical of normal galaxies (i.e., $\lesssim 10^{40} \text{ erg s}^{-1}$; see Figure 3; Hornschemeier et al. 2002, hereafter Paper VIII). Their average $\nu L_{15\mu\text{m}}$ luminosity of $\approx 6 \times 10^8 L_{\odot}$ is also typical of normal galaxies. These sources arise at smaller X-ray-to-optical flux ratios than the X-ray detected starbursts [i.e., $\log(\frac{L_X}{L}) \lesssim -2$]. Thus to detect higher redshift normal galaxies will require either deeper *Chandra* observations or the application of X-ray stacking techniques (e.g., Paper VIII).

Deeper IR observations (i.e., GOODS⁹) are planned with *SIRTF* over $\approx 160 \text{ arcmin}^2$ of the most sensitive region of the CDF-N: these should reach a depth in the $24 \mu\text{m}$ MIPS band to an equivalent $15 \mu\text{m}$ flux density of $\approx 10 \mu\text{Jy}$. In addition to providing a sample of ≈ 100 X-ray detected ELGs with $24 \mu\text{m}$ counterparts, these observations should be deep enough to detect counterparts for the majority of the X-ray detected ALGs and AGN-dominated sources.

ACKNOWLEDGMENTS

This work would not have been possible without the support of the entire *Chandra* and ACIS teams. We acknowledge the financial support of NASA grant NAS 8-38252 (GPG, PI), NSF CAREER award AST-9983783 (DMA, FEB, WNB, CV), NASA GSRP grant NGT5-50247 and the Pennsylvania Space Grant Consortium (AEH), and NSF grant AST-9900703 (DPS).

REFERENCES

- Akiyama, M., et al. 2000, *ApJ*, 532, 700
 Alexander, D.M., et al. 2001a, *ApJ*, 554, 18
 Alexander, D.M., Brandt, W.N., Hornschemeier, A.E., Garmire, G.P., Schneider, D.P., Bauer, F.E., & Griffiths, R.E. 2001b, *AJ*, 122, 2156 (Paper VI)
 Alexander, D.M., Vignali, C., Bauer, F.E., Brandt, W.N., Hornschemeier, A.E., Garmire, G.P., & Schneider, D.P. 2002, *AJ*, 123, 1149
 Aussel, H., Cesarsky, C.J., Elbaz, D., & Starck, J.L. 1999, *A&A*, 342, 313
 Aussel, H., et al. 2002, in preparation
 Barcons, X., Franceschini, A., De Zotti, G., Danese, L., & Miyaji, T. 1995, *ApJ*, 455, 480
 Barger, A.J., Cowie, L.L., Trentham, N., Fulton, E., Hu, E.M., Songaila, A., & Hall, D. 1999, *AJ*, 117, 2656
 Bauer, F.E., et al. 2002, in preparation
 Brandt, W.N., et al. 2001a, *AJ*, 122, 1 (Paper IV)
 Brandt, W.N., et al. 2001b, *AJ*, 122, 2810 (Paper V)
 Chary, R. & Elbaz, D. 2001, *ApJ*, 556, 562
 Cohen, J.G., Hogg, D.W., Blandford, R., Cowie, L.L., Hu, E., Songaila, A., Shopbell, P., & Richberg, K. 2000, *ApJ*, 538, 29
 Cohen, J.G. 2001, *AJ*, 121, 2895
 Cowie, L.L., Garmire, G.P., Bautz, M.W., Barger, A.J., Brandt, W.N., & Hornschemeier, A.E. 2002, *ApJ*, 566, L5
 Dawson, S., Stern, D., Bunker, A.J., Spinrod, H. & Dey, A. 2001, *AJ*, 122, 598
 Elbaz, D., Cesarsky, C.J., Chantal, P., Aussel, H., Franceschini, A., Fadda, D., & Chary, R.R. 2002, *A&A*, in press (astro-ph/0201328)
 Fadda, D., Flores, H., Hasinger, G., Franceschini, A., Altieri, B., Cesarsky, C., Elbaz, D., & Ferrando, P. 2002, *A&A*, in press (astro-ph/0111412)
 Garmire, G.P., et al. 2002, *ApJ*, submitted
 Gehrels, N. 1986, *ApJ*, 303, 336
 Giacconi, R., et al. 2001, *ApJ*, 551, 624
 Griffiths, R. E., Ptak, A., Feigelson, E. D., Garmire, G., Townsley, L., Brandt, W. N., Sambruna, R., & Bregman, J. N. 2000, *Science*, 290, 1325
 Hornschemeier, A.E., et al. 2001, *ApJ*, 554, 742 (Paper II)
 Hornschemeier, A.E., et al. 2002, *ApJ*, in press (astro-ph/0110094; Paper VIII)
 Lira, P., Ward, M., Zezas, A., Alonso-Herrero, A., & Ueno, S. 2002, *MNRAS*, 330, 259
 Moran, E.C., Lehnert, M.D., & Helfand, D.J. 1999, *ApJ*, 526, 649
 Rowan-Robinson, M. et al. 1997, *MNRAS*, 289, 490
 Schmidt, M., et al. 1998, *A&A*, 329, 495
 Stark, A.A., Gammie, C.F., Wilson, R.W., Bally, J., Linke, R.A., Heiles, C., & Hurwitz, M. 1992, *ApJS*, 79, 77
 Williams, R.E., et al. 1996, *AJ*, 112, 1335

⁷ We note that far-IR background and sub-mm source-count constraints restrict the number of possible Arp 220-type galaxies (e.g., Chary & Elbaz 2001).

⁸ The $I - K$ and $V - I$ colors were taken from the photometric catalog produced in Paper VI.

⁹ For details on GOODS, see <http://www.stsci.edu/science/goods/>.